Journal of Applied Fluid Mechanics, Vol. 14, No. 2, pp. 567-579, 2021.
Available online at www.jafmonline.net, ISSN 1735-3572, EISSN 1735-3645.
DOI: 10.47176/jafm.14.02.31482

Experimental Study on Slug Flow Characteristics and its Suppression by Microbubbles in Gas-Liquid Mixture Pipeline

T. Ling[1, 2], T. Wang[1], G. Lei[1], Z. Fang[2], L. Zhao[3] and C. Xu[2†]

[1] *State Key Laboratory of Technologies in Space Cryogenic Propellants, Beijing, 100028, China*
[2] *National Engineering Research Centre of Turbo-Generator Vibration, School of Energy and Environment, Southeast University, Nanjing, 210096, China*
[3] *CAS Key Laboratory of Low-Carbon Conversion Science and Engineering, Shanghai Institute of Advanced Studies, Chinese Academy of Sciences, Shanghai, 201210, China*

†*Corresponding Author Email: chuanlongxu@seu.edu.cn*

(Received February 15, 2020; accepted August 6, 2020)

ABSTRACT

In the oil-gas mixture transportation system of offshore oilfields, it is of great theoretical and practical significance to study the flow characteristics of the slug flow and its suppression or elimination. In this paper, the characteristics of the slug flow and microbubbles in a laboratory-scale rig are experimentally studied and analyzed by a multi-parameters measurement system including electrical resistance tomography (ERT), high-speed camera, and traditional pressure sensor. The suppression of the microbubbles on the slug flow formation is further investigated. Experimental results showed that the bubbles with different sizes from the microbubble generator have different aggregation and dispersion characteristics. The microbubbles can suppress the formation of the slug flow by increasing the liquid slug pressure and further affect the motion of the slug by enhancing the disturbance effect of the boundary layer, so as to achieve the suppression on slug flow.

Keywords: Slug flow; Microbubbles; Electrical resistance tomography; High-speed imaging; Suppression.

1. INTRODUCTION

With the growth of energy demand, petroleum extraction has been gradually expanding from land oil fields to offshore oil fields. The produced outputs in offshore oilfields are generally a multiphase mixture of oil and gas. The multiphase mixture is mainly transported to land by oil-gas separation transportation and oil-gas mixture transportation. Among them, in the oil-gas mixture transportation system, the oil and gas mixture are directly transported from the deep sea to offshore oil production platforms through pipelines, which can reduce the construction cost of offshore oil production equipment and is widely used in the offshore oil industry (Pedersen *et al.* 2017; Zheng *et al.* 1995). However, in the process of oil-gas mixture transportation, severe slug flow may occur due to the changes of operating conditions and the structures of the vertical and inclined upward pipelines in the transportation system. The slug flow is a very complex multiphase flow process, which usually illustrates that the liquid slug and long bubble alternately flow through the pipeline. As a consequence, the flow rate and pressure in the pipeline fluctuate sharply. The fluctuations cause intermittent fluid stress to impact the transportation pipeline, which may lead to the shutdown or damage of the downstream transportation equipment in the transportation system of oil and gas mixture in some severe cases. Therefore, it is of great theoretical and practical significance to study the flow characteristics of slug flow and its suppression or elimination (Li *et al.* 2013; Zhang *et al.* 2015).

In past decades, many researches on slug flow have been performed, and various models and empirical formulas have been proposed to calculate the characteristic parameters of slug flow (Xie *et al.* 2017; Luo, 2007; Momen *et al.* 2016), such as slug flow pressure gradients, slug gas fraction, and slug occurrence frequency. Based on the conservation laws of mass and momentum, Dukler and Hubbard (1975) proposed a model of slug flow in a horizontal pipe, which is capable of calculating the flow pressure drop and the average cross-section gas fraction. Different from the traditional homogeneous model and split-phase model, the

model takes the influence of flow pattern into account when calculating pressure drop, and thus has good adaptability to slug flow. Nicholson *et al.* (1978) further proposed the empirical formula to calculate the frequency and gas fraction of liquid slug to optimize the unit-body model, so as to realize the closure of control equations. But the effects of pressure drop and hydraulic jump in the liquid membrane area were not considered in the model. Gregory and Scott (1969) used carbon dioxide and water as experimental media to study the slug flow in a horizontal pipe, and verified that the occurrence frequency of liquid slug increases with increasing the slug velocity. An empirical formula for calculating the slug frequency was further proposed through the analysis of experimental data. However, in the empirical formula, only the effects of pipe diameter and fluid flow velocity were considered, and the impacts of fluid viscosity and density were ignored. Taitel *et al.* (1977) obtained an empirical formula for calculating the occurrence frequency of slugs through dimensionless analysis and proposed that the generation mode of slug flow would affect the occurrence frequency of slugs. These models for characteristic parameters of slug flow provides the basis of the in-depth insight into slug flow and the design of the pipeline and downstream equipment in the transportation system of oil and gas mixture. However, the accuracy of these models and empirical formulas are limited in laboratory conditions and need to be verified in the industrial transportation process of the oil and gas mixture. The complex characteristics of slug flow also pose significant challenges to its measurement techniques. The pressure and gas fraction are the two main parameters used for the study of slug flow. The pressure sensors are used for pressure signal measurement, and the measurement techniques for gas fraction measurement mainly includes the conductance probe (Liu, 2011), gamma-ray densitometer (Wang *et al.* 2005), and electrical tomography (Wang and Wu, 2009; Wang *et al.* 2019). The conductance probe is intrusive, which disturbs the flow pattern of the slug flow. Moreover, it can only measure the gas fraction of a single-point in slug flow, and couldn't characterize the slug flow in 2D/3D space. Gamma-ray densitometer uses the attenuation of the radioactive density for slug flow measurement due to the different absorption properties of gas and liquid. It has the advantages of high accuracy and non-intrusiveness, but is expensive in equipment and has certain safety risks. In contrast, electrical tomography has gradually been widely used for the measurement and characterization of multiphase flow due to its advantages of non-invasiveness, low cost, and 2D visualization. Among electrical tomographic techniques, the electrical resistance tomography technique has been applied in bubble bed (Jin *et al.* 2007) and flotation bed (Vadlakonda and Mangadoddy, 2017). Few works have been reported that tomographic techniques have been applied to characterize the slug flow. Presently, it is very urgent to develop advanced measurement techniques for the characterization of slug flow.

Many researches have also been performed on the suppression or elimination of slug flow in the past two decades. Schmidt *et al.* (1979) proposed a throttling technique to eliminate severe slug flow, which is simple and easy to operate. However, the throttling technique will generate considerable back pressure and increase the pressure of the upstream pipeline at the throttling point, resulting in the decline of oil well production. Jansen *et al.* (1996) proposed the gas-lift method to eliminate severe slug. Nevertheless, the gas injection is costly, and the injection of large amounts of gas will also reduce oil production. Johal *et al.* (1997) used the multi-phase pump to eliminate severe slug flow, and the actual effect is closely related to the type and location of the pump, making it difficult to operate. Almeida *et al.* (1998) presented the perturbation method to suppress severe slug. A venturi was installed at the bottom inlet of the vertical pipeline to prevent liquid accumulation, thereby suppressing the occurrence of severe slug. However, it is difficult to maintain the flow state after disturbances. Therefore, it is of great significance to propose a slug flow suppression method with high feasibility and low operating cost.

The diameter of microbubbles is less than 50 μm, which is characterized by small bubble size, large specific surface area, high adsorption efficiency, and slow rising speed in liquid. The microbubbles can effectively separate solid impurities, rapidly improve oxygen concentration, kill harmful bacteria in water, and reduce solid-liquid interface friction coefficient. Presently, the microbubbles are widely used in the fields of air flotation water purification (Takahashi *et al.* 2003), high-precision transmission (Cravotto and Cintas, 2007), and micro-bubble drag reduction (Stephani and Goldstein, 2010). It has also shown certain technical advantages and good application prospects in the fields of sewage and wastewater treatment, groundwater and soil environment restoration. Based on the characteristics mentioned above, microbubbles are introduced into the suppression of slug flow. The microbubbles will affect the back-mixing flow in the boundary layer during the movement of slug flow (Zhao *et al.* 2018; Mashhadani *et al.* 2011; Li *et al.* 2016), which is expected to play a role in slug flow suppression.

In this paper, a multi-parameters measurement system consisting of electrical resistance tomography (ERT), high-speed camera, and traditional pressure sensor is proposed, which can avoid the invasive weakness of traditional gas-liquid two-phase flow measurement method. The flow characteristics of typical slug flow and the microscopic features of microbubbles are further studied experimentally. Moreover, the suppression effect of microbubbles on slug flow is studied experimentally on a laboratory-scale rig. The influences of the microbubbles on gas fraction, pressure, and occurrence period of slug flow at different operation conditions are investigated. Finally, a suppressing method for slug flow by microbubbles, with high feasibility and low

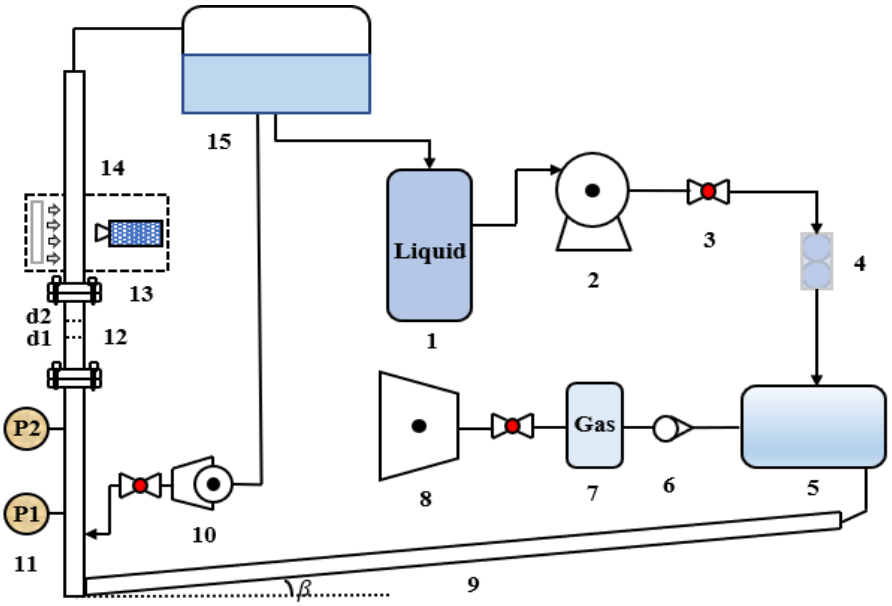

(a) Schematic diagram：1-liquid tank；2- water pump；3-check valve；4-liquid flowmeter；5- baffle-type gas-liquid mixing tank；6- gas flowmeter；7-gas tank；8- air compressor；9- horizontal inclined pipe；10- microbubble generator；11 - pressure gauges；12-ERT sensor；13- high-speed camera and backlight syst；14-vertical pipe；15- gas-liquid separation tank

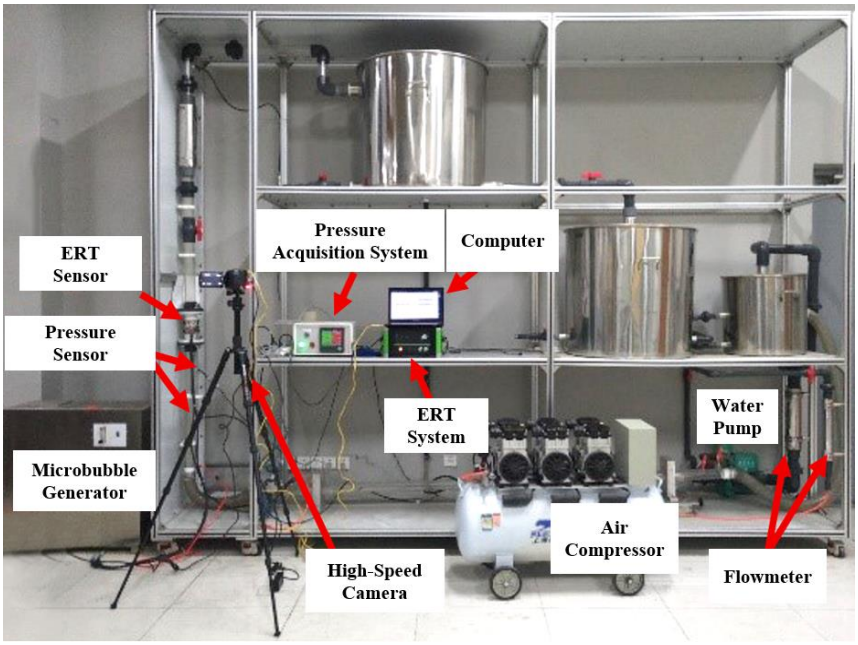

(b) Photograph

Fig. 1. Experimental rig of slug flow.

operating cost compared to previous schemes proposed by scholars, is further presented.

2. EXPERIMENTAL RIG

Figure 1 shows the laboratory-scale experimental rig of slug flow. In the baffle-type gas-liquid mixing tank, the air from the air compressor and the water produced by the liquid pump are mixed. The mixed gas-liquid two-phase flow enters the horizontal inclined pipeline and flows into the vertical pipe. The output of the microbubble generator is connected with the bottom of the vertical pipeline or the end of the horizontal inclined pipeline, where the gas-liquid two-phase flow is mixed with the microbubbles. Then the gas-liquid two-phase flow from the vertical pipeline enters the gas-liquid separation tank for gas-liquid separation, in which the air is directly emptied, and the separated water flows into the liquid tank from the bottom of the

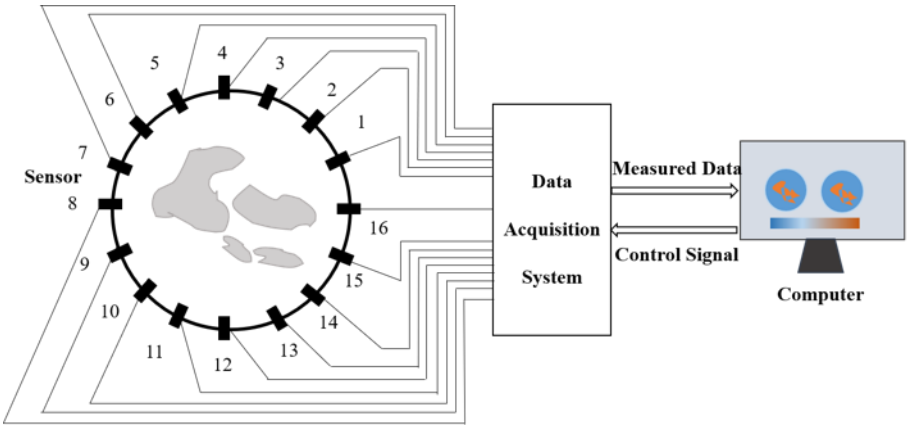

Fig. 2. Schematic of ERT system.

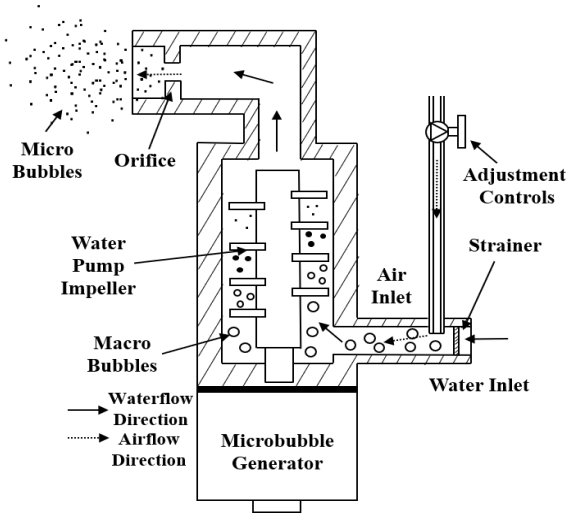

Fig. 3. Schematic diagram of microbubble generator.

tank. The horizontal inclined and vertical transparent plexiglass pipes have an inner diameter of 50 mm and are connected by a hose. The lengths of the horizontal inclined pipe and the vertical pipe are 3 m and 2.5 m, respectively. The adjustable angle range of the inclination pipeline (β) is 1 to 5°.

A comprehensive measurement system for complex flow characteristics of slug flow is presented by combining electrical resistance tomography, pressure sensor, and high-speed camera, which can achieve the simultaneous measurement of flow pressure and gas fraction, slug flow visualization and cross-section gas-liquid distribution. The pressure transmitter PT218 with the accuracy of 0.5% FS and sampling rate of 10Hz is used to monitor the slug flow pressure. The high-speed camera Phantom M/R/LC110 (resolution 1280*800 px, sampling rate 1630 frames/s) is used for visualization of slug flow, and electrical resistance tomography (ERT, ITS P2000) is used to real-time detection of gas fraction over the cross-section of pipeline, respectively. Figure 2 shows a schematic of the ERT system. It consists of a sensor array, a data acquisition system, and a tomographic algorithm in computer. The liquid phase and gas phase have the different conductivities, and ERT system can measure and reconstruct the conductivity distribution of gas-liquid medium in its sensing field, and then obtain the actual cross-sectional distribution of the gas-liquid mixture.

Microbubbles are generated by the dissolved release gas method (Luo, 2007). The schematic diagram of the microbubble generator is shown in Fig. 3. The gas and liquid are accurately controlled and mixed in a certain ratio, and the gas-liquid mixture is sent to the pump. In the pump, the impeller pressurizes the gas-liquid two-phase flow through high-speed rotation to promote the dissolution of the gas. The supersaturated liquid, which dissolves a large amount of gas, flows to the outlet of the generator and releases the gas through the orifice to form the microbubble solution. The generated microbubble solution takes more than 1minute from the turbidity to the clarification under static condition, which can ensure that the microbubble will not disappear due to the coalescence or dissolution in sufficient experimental time.

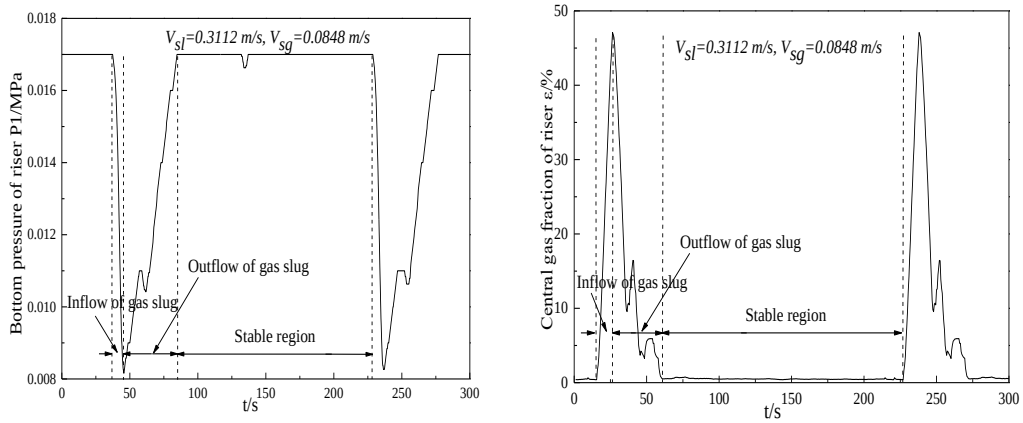

(a) Pressure fluctuations for severe slug flow pattern (b) Gas fraction fluctuations for severe slug flow pattern

Fig. 4. Variation of pressure and gas fraction of slug flow with time at the gas-liquid ratio of 0.27.

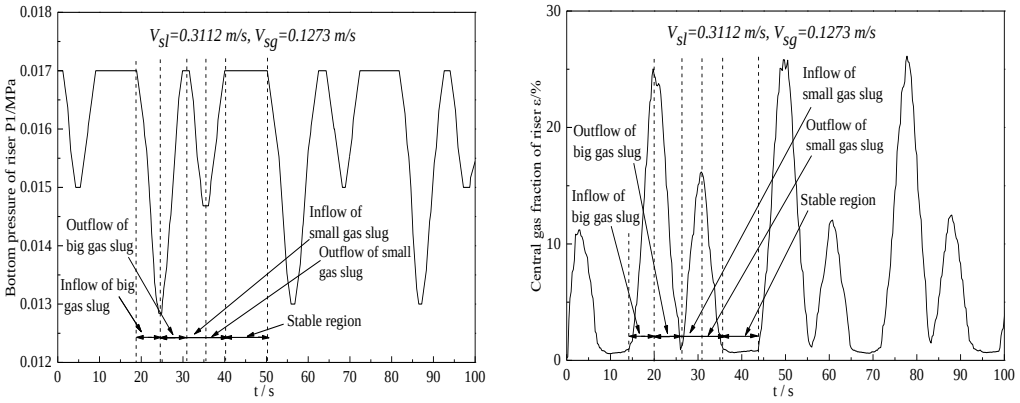

(a) Pressure fluctuations for transitional slug flow pattern (b) Gas fraction fluctuations for transitional slug flow pattern

Fig. 5. Variations of pressure and gas fraction of slug flow at the gas-liquid ratio of 0.41.

3. CHARACTERISTICS OF SLUG FLOW AND MICROBUBBLES

3.1 Typical Flow Patterns of Slug Flow

Experiments on slug flow patterns are conducted at different operating conditions. In experiments, the angle of the inclination pipeline (β) is 3°. The superficial liquid velocity V_{sl} ranges from 0.0849 m/s to 0.6508 m/s, and the superficial gas velocity V_{sg} is in the range of 0.0848 m/s~1.2732 m/s.

Figure 4 shows the variation of the pressure and gas fraction of slug flow with time at the gas-liquid ratio of 0.25. It can be seen from Fig. 4 that at low gas-liquid ratios (the ratio of superficial gas velocity and superficial liquid velocity) (e.g., 0.27), the pressure fluctuations and changes in gas fraction obtained by ERT present a typical severe slug flow pattern, and the pressure fluctuations of slug flow are complementary to the fluctuations of the gas fraction. Since the ERT sensor and the pressure sensor are not located on the same cross-section of the pipeline, the measured pressure and gas fraction signals have a time offset. The pressure fluctuations at the bottom of the vertical pipe have three stages. In the first stage, the pressure starts to drop sharply with the inflow of the gas slug, and in the second stage, with the outflow of the gas slug, the liquid slug starts to flow into the vertical pipe, and the pressure rises rapidly. Finally, in the third stage, the pressure reaches a maximum and then remains stable for a period of time until the next gas slug enters and forms a new cycle. Due to the long accumulation time of the gas at the bottom of the horizontal elbow, the pressure in the vertical pipe has large fluctuation, resulting in a strong impact of the intermittent fluid stress on the transportation pipeline. Correspondingly, the gas fraction measured by ERT increases rapidly at first and then decreases sharply, indicating that the shape of the gas slug is severely disturbed by the boundary layer.

Figure 5 shows the variation of pressure and gas fraction of slug flow with time at the gas-liquid ratio of 0.41. From Fig. 5, at high gas-liquid ratios

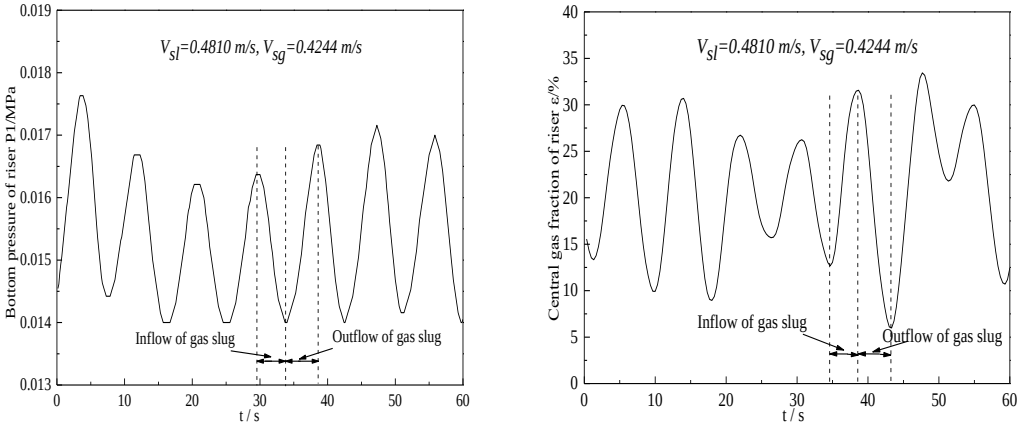

(a) Pressure fluctuations for bullet-like slug flow pattern (b) Gas fraction fluctuations for bullet-like slug flow pattern

Fig. 6. Variations of pressure and gas fraction of slug flow with time at the gas-liquid ratio of 0.88.

(a) Head of the gas slug (b) Tail of the gas slug

Fig. 7. Images of the gas slug by high-speed camera for V_{sl} =0.4810 m/s and V_{sg} =0.4244 m/s.

(e.g., 0.41), the pressure and gas fraction fluctuations present a transitional slug flow pattern. It can be found that with the increase of gas-liquid ratio, the long gas slug is decomposed into two small gas slugs. Correspondingly, there are two gas slug inflow and two gas slug outflow processes, and a stable liquid slug region in the transitional slug flow. Yet the transitional slug flow is not stable. As the gas-liquid ratio increases, the number of gas slugs increases, and eventually develops into a bullet-like slug flow at higher gas-liquid ratio (e.g., 0.88) corresponding to Fig. 6. From Fig. 6, the frequency of the bullet-like slug is high, and the stable region of pressure fluctuation becomes shorter or even disappears. As a consequence, the impact of pressure fluctuations on the transportation pipeline correspondingly becomes weak. From Figs. 4-6, when severe slug flow at a low gas-liquid ratio occurs, the pressure fluctuation in the vertical pipeline is large due to the long-time gas accumulation at the bottom of the horizontal elbow, resulting in a large impact of the intermittent fluid stress on the pipeline. In the extreme condition of severe slug flow, the vertical pipe is empty or full of water, and its characteristic parameters such as gas fraction and pressure are of little significance. However, at the high gas-liquid ratio, the bullet-like slug flow has a high occurrence frequency, and the pressure fluctuation is small, and the corresponding stress impact on the pipeline is weak. Therefore, the paper will focus on the characteristics of bullet-like slug flow. To simplify the description, the slug flow refers to the bullet-like slug flow in the following sections.

The motion of the slug flow is visualized by ERT and a high-speed camera. Figure 7 shows the high-speed camera images of the slug for V_{sl}=0.4810 m/s and V_{sg}=0.4244 m/s. It can be seen from Fig. 7 that the head of the gas slug is compressed into a flat

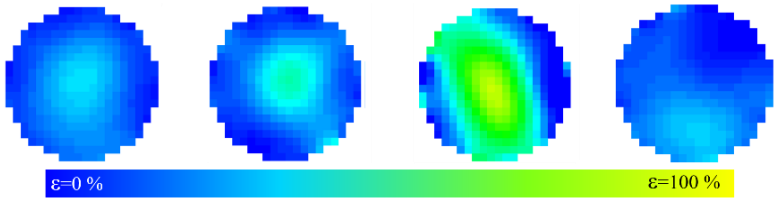

(a) 0 s (b) 0.25 s (c) 1 s (d) 2 s

Fig. 8 Cross-sectional distribution of gas fraction by ERT for V_{sl}= 0.4810 m/s and V_{sg}= 0.4244 m/s.

shape by the large liquid slug pressure, the side of the gas slug is obviously undular because of the disturbance of the boundary layer, and the tail of the slug is squeezed narrow due to the back mixing of the boundary liquid. The gas slug presents the shape of an inverted bullet with a round head and tail tip, which is defined as the bullet-like slug. Figure 8 shows the cross-sectional distribution of the gas fraction measured by ERT at different times. From Fig. 8 (a) and 8 (b), the gas fraction gradually increases when the gas slug head enters the ERT sensor. In Fig. 8 (c), the main body of gas slug passes through the sensor, and thus the gas fraction reaches the maximum. Contrarily, in Fig. 8 (d), the tail section of the gas slug is about to leave the sensor, and the corresponding gas fraction sharply decreases. The ERT measurement results in the entire cycle of gas slug are consistent with the visualization of the high-speed camera.

3.2 Characteristics of Microbubbles

Figure 9 shows the microbubble image in a vertical pipe taken by a 1X magnification lens. It can be seen from Fig. 9 that the microbubbles produced by microbubble generationer are full of vertical pipe and has a high concentration, and the vertical pipe presents the state of milky white mist. At the same time, there are a lot of bubbles adhered to the inner wall surface of the vertical pipe.

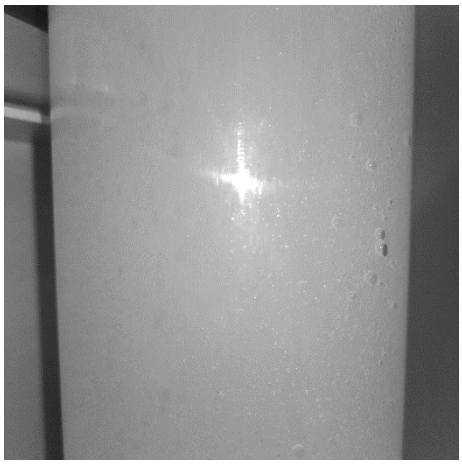

Fig. 9. Microbubble image in a vertical pipe.

In experiments, it was found that the microbubbles in the vertical pipe are easily flushed by water fluid, and yet many microbubbles are still attached to the inner wall of the pipe. Thus, the microbubbles of the generator can be characterized by analyzing the images of the microbubbles attached to the pipe wall. After the microbubbles in the vertical pipe are flushed away, the microbubbles adhered to the wall are photographed by the macro lenses with 18X and 36X magnification, respectively, as shown in Fig. 10. From Fig. 10, a large number of bubbles are adhered to the wall of the pipe due to the effect of surface tension, and the sizes of the bubbles are different. Figure 11 shows the statistical bubble size distribution on the wall. It can be seen from Fig. 11 that the bubbles with different sizes on the wall have different aggregation and dispersion characteristics. The proportion of microbubbles with the diameter less than or equal to 50 μm is 14.16%, most of which are in a free state, indicating that microbubbles are not easy to aggregate. The low proportion also indicates that microbubbles have lower surface tension. The proportion of bubbles with the diameter between 50 and 100 μm is 29.22%, and it is readily adsorbed by the large bubbles with a size of more than 1 mm. The proportion of the bubbles with the size larger than 100 μm is nearly 50%, and these bubbles are mainly in a free state.

4. Experimental Study Of Suppression Of The Microbubbles On Slug Flow

In this paper, the effects of microbubbles on the flow characteristics of slug flow at different gas-liquid ratios (Superficial gas velocity V_{sl}=0.1981 m/s~0.6508 m/s, Superficial liquid velocity V_{sg}=0.1273 m/s~1.2732 m/s) are experimentally studied. Moreover, to study the influence of microbubble inflow position in the gas-liquid mixture pipeline, two inlets (a and b) at the bottom of the vertical pipe and near the elbow of the horizontal inclined pipe are chosen, respectively, as shown in Fig. 12.

Figure 13 shows the comparison of the images of the slug flow with or without microbubbles taken by the high-speed camera. From Fig. 13(a), it can be seen that the gas slug without microbubbles has a clear boundary, while the gas slug boundary in Fig. 13(b) with microbubbles becomes blurry. It is concluded that the incoming microbubbles form a large number of bubbles in the boundary layer, and have effects on the motion of gas slug flow.

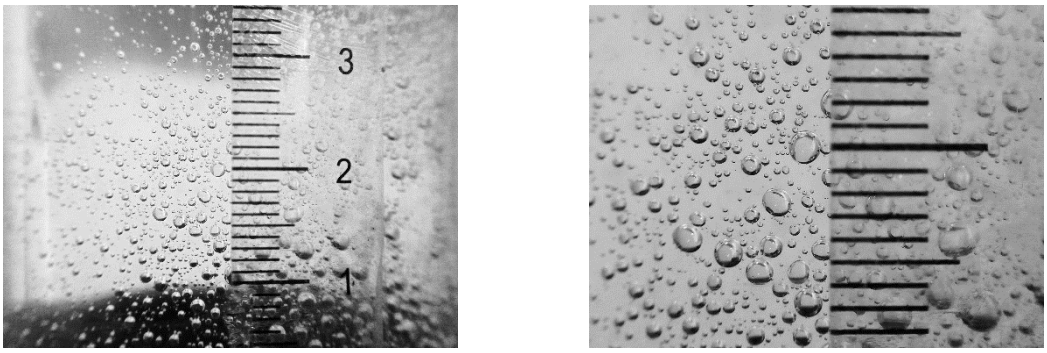

(a) Bubble distribution with 18X lens (b) Bubble distribution with 36X lens

Fig. 10. Bubbles distribution in the vertical pipe wall.

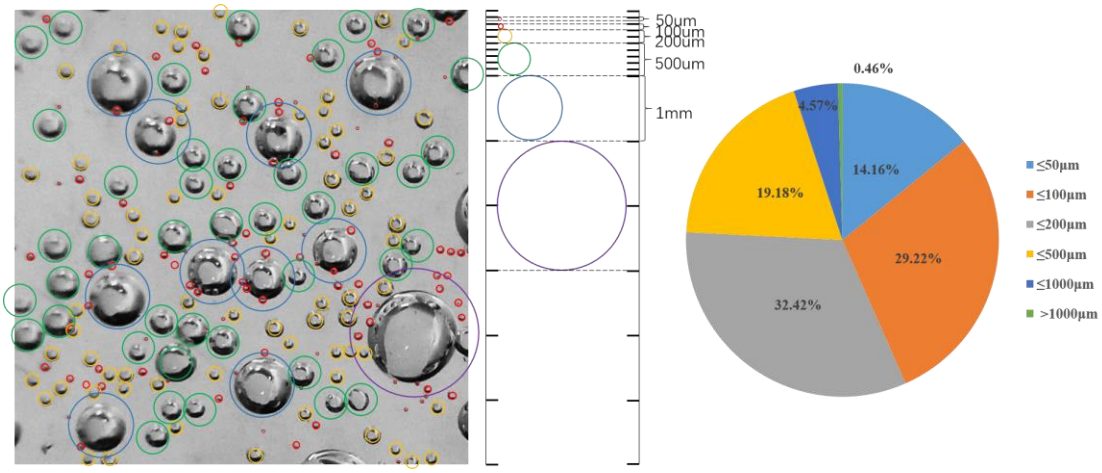

Fig. 11. Statistical bubble size distribution.

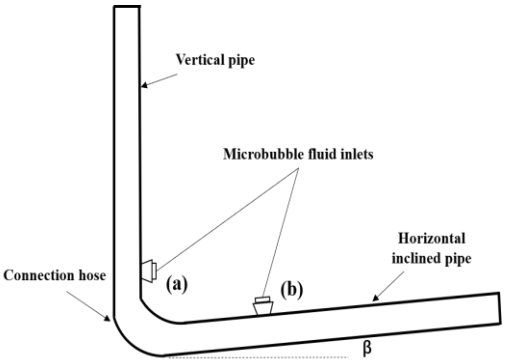

Fig. 12. Schematic diagram of microbubble inlets.

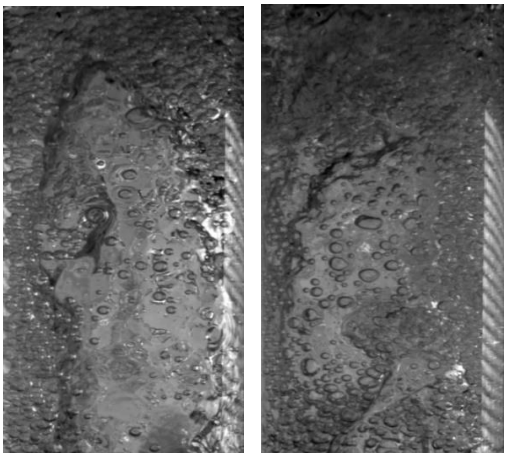

(a) Without microbubbles (b) With microbubbles

Fig. 13. High-speed camera images of the gas slug for V_{sl} =0.4810 m/s and V_{sg} =0.5659 m/s.

4.1 Effect of Microbubbles on Gas Fraction and Pressure of Slug Flow

Figure 14 shows the probability density function (PDF) of the gas fraction rate (ε) of slug flow under three experimental conditions (without microbubbles (slug), microbubbles introduced at the bottom of the vertical pipe (vertical), and microbubbles introduced near the elbow of the horizontal inclined pipe (horizontal)). The superficial liquid velocity V_{sl} is 0.3122m/s, and the superficial gas velocity V_{sg} ranges from 0.1273 m/s to 1.2732 m/s.

From Fig.14, when the superficial gas velocity V_{sg} is 0.1273 m/s, the probability density distribution of the gas fraction of the slug flow is unimodal. The introduction of microbubbles causes the peak of the PDF of the gas fraction to move to the left side of the liquid slug region. When the superficial gas velocity V_{sg} is 0.7074 m/s, the gas fraction

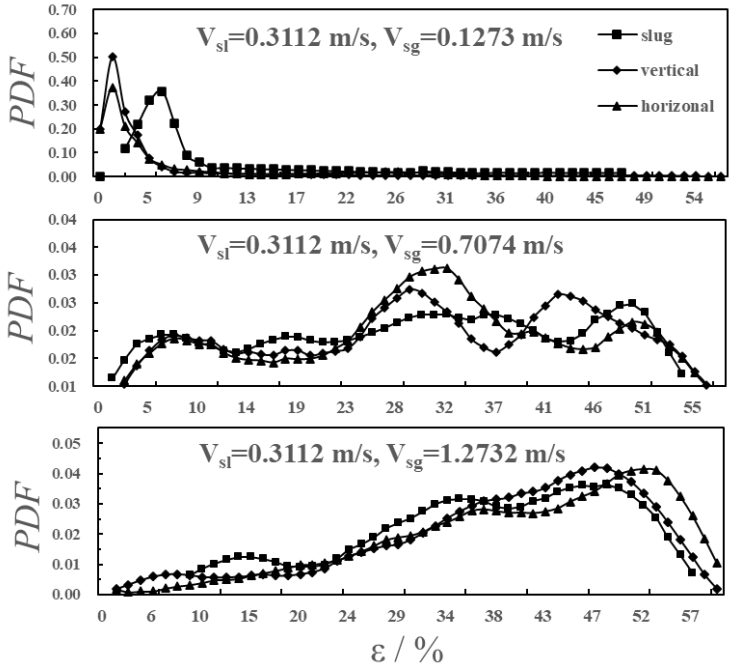

Fig. 14. Probability density function of the gas fraction.

fluctuation of slug flow presents a multi-peak distribution, and the introduction of microbubbles increases the diversity of the peaks of the PDF in the right gas-slug region, and the multi-peaks are clearly recognized. When the superficial gas velocity V_{sg} increases to be 1.2732 m/s, the multimodal distribution of the PDF in the high gas fraction region recloses to a unimodal distribution since the gas slugs play a leading role. The introduction of microbubbles promotes the peak of the PDF to move to the right side (the gas slug region). From the above discussion, the introduction of microbubbles will cause a change in the probability density distribution of slug gas fraction. In the liquid slug region, the microbubbles lead to the unimodal and narrow peak of the probability density distribution of gas slug, indicating that microbubbles contribute to the coalescence of the liquid slugs to some extent.

Figure 15 shows the probability density function of the pressure of slug flow under three experimental conditions. It can be seen that when the superficial gas velocity V_{sg} is 0.1273 m/s, the probability density fluctuation of the pressure presents a typical unimodal distribution. The introduction of microbubbles causes the movement of the peaks to the high-pressure region. When the superficial gas velocity V_{sg} is 0.7074 m/s, the pressure corresponding to the peak decreases significantly, and at the same time, two more low peaks appear in the low-pressure region. Notably, the peak in the high-pressure region under vertical condition decreases significantly, and the peak in the low-pressure area increases significantly when the microbubbles are introduced at the bottom of the vertical pipe. When the gas velocity further increases to be 1.2732 m/s, the pressure fluctuation without microbubbles is still dominated by a single peak distribution, while those at the conditions of microbubbles introduced at the bottom of the vertical pipe and near the elbow of the horizontal inclined pipe are characterized as a multi-peak distribution, indicating that the introduction of microbubbles enhances the pressure fluctuation.

4.2 Effect of Microbubbles on the Occurrence Period (Frequency) of Slug Flow

Figure 16(a) shows the variation of the occurrence period of the slug flow with the superficial gas velocity at a given superficial liquid velocity. The superficial liquid velocity V_{sl} is 0.481m/s, and the superficial gas velocity V_{sg} ranges from 0.3112 m/s to 1.4147 m/s. Figure 16(b) shows the variation of the occurrence period of the slug flow with the superficial liquid velocity at a given superficial gas velocity. The superficial gas velocity V_{sg} is 0.4244m/s, and the superficial liquid velocity V_{sl} is in the range of 0.0849 m/s-0.6366 m/s. It can be seen that the occurrence period of the slug flow is prolonged significantly with microbubbles introduced at the bottom of the vertical pipe. The introduction of the microbubbles changes the flow state of the slug flow from the elbow tube of the horizontal inclined pipe, thus reducing the occurrence frequency of the slug flow. However, the microbubbles introduced near the elbow of the horizontal inclined pipe have a slight effect on the slug flow characteristics. As a consequence, the slug occurrence period without microbubbles and with microbubbles introduced near the elbow of the horizontal inclined pipe is very close. In conclusion, the microbubbles introduced at the bottom of the vertical pipe has a significant suppression effect on the occurrence frequency of slug flow.

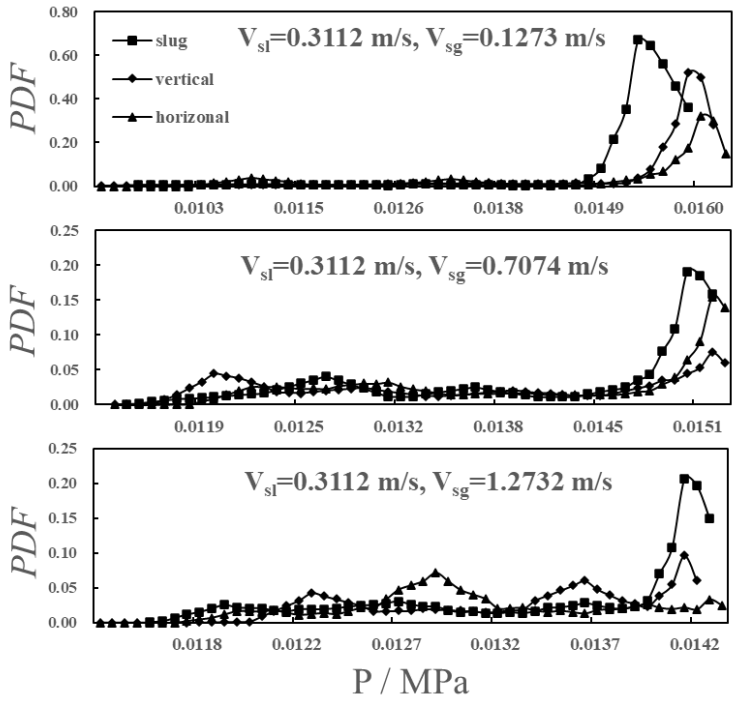

Fig. 15. Probability density function of the pressure of slug flow.

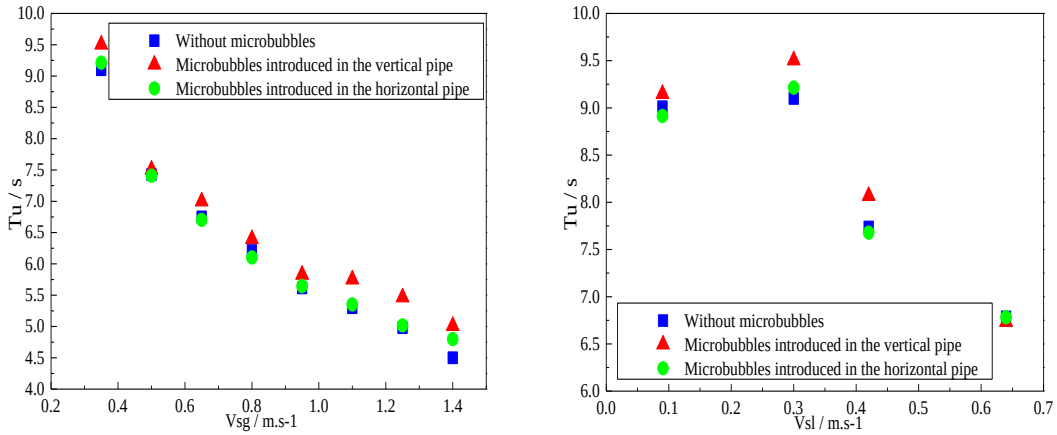

(a) Variation with superficial gas velocity (b) Variation with superficial liquid velocity

Fig. 16. Variation of the occurrence period of slug flow.

Table 1 Error analysis

Experimental Conditions	Gas Fraction / %	Relative Error /%	Pressure / MPa	Relative Error /%	Occurrence Period /s	Relative Error /%
Slug	22.49	6.84	0.0146	7.14	7.49	8.28
Vertical	21.14	9.62	0.0156	9.53	7.48	9.89
Horizontal	20.78	9.73	0.0154	9.26	7.51	9.75

The errors of three kinds of experiments were analyzed for V_{sl}=0.0849 m/s and V_{sg}=0.7074 m/s, and the results are summarized in Tab.1. The mean values of gas fraction, pressure, and occurrence period and their relative errors are displayed. The maximum error is within 10%, indicating that the measured parameters are reliable.

4.3 Suppression of Microbubbles on the Slug Flow

Experiments were further carried out to study the suppression effect of the microbubbles introduced in the vertical pipe under different gas-liquid ratios (η). The experimental conditions are summarized in Tab. 2.

Table 2 Experimental conditions

η	V_{sl} / m.s^{-1}	V_{sg} / m.s^{-1}	η	V_{sl} / m.s^{-1}	V_{sg} / m.s^{-1}
0.7	0.6508	0.4244	4.1	0.3112	1.2732
0.9	0.4810	0.4244	4.5	0.3112	1.4147
1.2	0.4810	0.5659	5.0	0.0849	0.4244
1.4	0.3112	0.4244	6.7	0.0849	0.5659
1.8	0.3112	0.5659	8.3	0.0849	0.7074
2.3	0.3112	0.7074	10.0	0.0849	0.8488
2.7	0.3112	0.8488	11.7	0.0849	0.9903
3.2	0.3112	0.9903	13.3	0.0849	1.1318
3.6	0.3112	1.1318	16.7	0.084883	1.4147

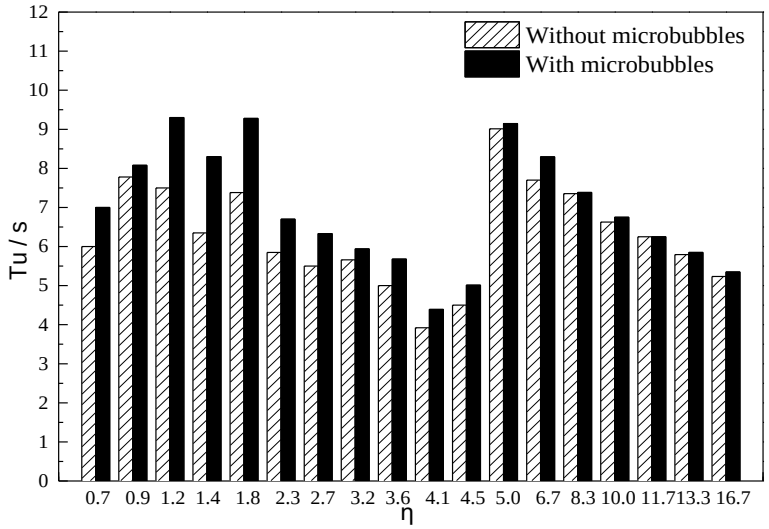

Fig. 17. Influence of the microbubbles on the occurrence period of slug flow at different gas-liquid ratios.

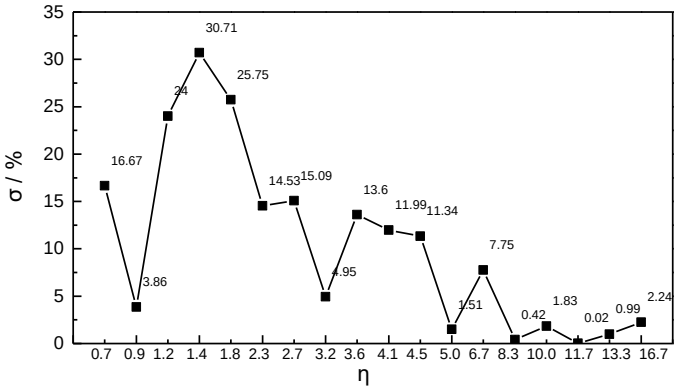

Fig. 18. Influence of the microbubbles on the percentage growth of slug occurrence period at different gas-liquid ratios.

Figure 17 shows the influence of microbubbles on the occurrence period of slug flow at different gas-liquid ratios. It can be seen that at the same gas-liquid ratio, the average period of slug flow with microbubbles introduced becomes long. This indicates that the occurrence frequency of the slug flow decreases, and thus the microbubbles have a suppression effect on the occurrence of the slug flow. Figure 18 shows the influence of the microbubbles on the percentage growth (σ) of the slug occurrence period at different gas-liquid ratios. It can be seen that the suppression effect is most significant at the gas-liquid ratio of 1.2, 1.4, and 1.8, while at high gas-liquid ratio, the suppression

effect on the slug occurrence period is relatively weak.

From the above-mentioned experimental results, at a low gas-liquid ratio, the characteristics of slug flow would be affected by the microbubbles introduced at the bottom of the vertical pipe. The microbubbles can suppress the formation of the slug flow by increasing the liquid slug pressure and further affect the motion of the slug by enhancing the disturbance effect of the boundary layer, so as to achieve the suppression on slug flow.

5. CONCLUSION

In this paper, a multi-parameters measurement system consisting of electrical resistance tomography (ERT), high-speed camera, and traditional pressure sensor has been presented to characterize the slug flow and the microscopic features of microbubbles. The influences of microbubbles on the gas fraction, pressure, and occurrence period of slug flow at different operation conditions were further investigated in a laboratory-scale experimental rig. Experimental results showed that the introduction of microbubbles can promote the coalescence of the liquid slugs, enhance the pressure fluctuation of slug flow. And the microbubbles introduced at the bottom of the vertical pipe has a significant suppression effect on the occurrence frequency of slug flow by increasing the liquid slug pressure and further affect the motion of the slug by enhancing the disturbance effect of the boundary layer, while the suppression effect of microbubbles introduced near the elbow of the horizontal inclined pipe is relatively weak.

ACKNOWLEDGEMENTS

The authors wish to express their gratitude to the National Natural Science Foundation of China (No. 51676044) and the fund of the State Key Laboratory of Technologies in Space Cryogenic Propellants (No. SKLTSCP1908).

REFERENCES

Al-Mashhadani, M. K. H., H. C. H. Bandulasena, and W. B. Zimmerman (2011). CO2 mass transfer induced through an airlift loop by a microbubble cloud generated by fluidic oscillation. *Industrial & Engineering Chemistry Research* 51(4), 1864-1877.

Almeida, A. and M. Goncalves (1999). "Venturi for severe slug elimination", *9th International Conference on Multiphase 99 - Frontier Technology Comes of Age*, Lyon, France, pp. 149-158.

Cravotto, G. and P. Cintas (2007). Forcing and controlling chemical reactions with ultrasound. *Angewandte Chemie International Edition* 46(29), 5476-5478.

Dukler, A. E. and M. G. Hubbard (1975). A model for gas-liquid slug flow in horizontal and near horizontal tubes. *Industrial & Engineering Chemistry Fundamentals* 14(4), 337-347.

Gregory, G. A. and D. S. Scott (1969). Correlation of liquid slug velocity and frequency in horizontal cocurrent gas-liquid slug flow. *AIChE Journal* 15(6), 933-935.

Jansen, F. E., O. Shoham and Y. Taitel (1996). The elimination of severe slugging—experiments and modeling. *International journal of multiphase flow* 22(6), 1055-1072.

Jin, H., M. Wang and R. A. Williams (2007). Analysis of bubble behaviors in bubble columns using electrical resistance tomography. *Chemical Engineering Journal* 130(2-3), 179-185.

Johal, K. S., C. E. Teh and A. R. Cousins (1997). An alternative economic method to riserbase gas lift for deep water subsea oil/gas field developments//Offshore Europe. *Society of Petroleum Engineers* 38(5), 41.

Li, W., J. Gong, X. Lü, J. Zhao, Y. Feng and D. Yu (2013). A study of hydrate plug formation in a subsea natural gas pipeline using a novel high-pressure flow loop. *Petroleum science* 10(1), 97-105.

Li, X., H. Xu, J. Liu, *Zhang*, J. Li and Z. Gui (2016). Cyclonic state micro-bubble flotation column in oil-in-water emulsion separation. *Separation and Purification Technology* 165, 101-106.

Liu, X. (2011). Severe slugging prediction and elimination in offshore multiphase pipelines. Beijing：China University of Petroleum (in Chinese).

Luo, X. (2007). *Study on the flow characteristics of gas-liquid two-phase slug flow and gas-water three-phase slug flow*. Shandong: China University of Petroleum (in Chinese).

Momen, A. M., S. A. Sherif and W. E. Lear (2016). An analytical-numerical model for two-phase slug flow through a sudden area change in microchannels. *Journal of Applied Fluid Mechanics* 9(4), 1839-1850.

Nicholson, M. K., K. Aziz and G. A. Gregory (1978). Intermittent two phase flow in horizontal pipes: predictive models. *The Canadian Journal of chemical engineering* 56(6), 653-663.

Pedersen, S., P. Durdevic and Z. Yang (2017). Challenges in slug modeling and control for offshore oil and gas productions: A review study. *International Journal of Multiphase Flow* 88, 270-284.

Schmidt, Z., J. P. Brill and H. D. Beggs (1979). Choking can eliminate severe pipeline slugging. *Oil and Gas Journal* 11(12), 230-238.

Stephani, K. A. and D. B. Goldstein (2010). An examination of trapped bubbles for viscous

drag reduction on submerged surfaces. *Journal of Fluids Engineering* 132(4), 041303.

Taitel, Y. and A. E. Dukler (1977). A model for slug frequency during gas-liquid flow in horizontal and near horizontal pipes. *International Journal of Multiphase Flow* 3(6), 585-596.

Takahashi, M., T. Kawamura, Y. Yamamoto, H. Ohnari, S. Himuro and H. Shakut*sui* (2003).Effect of shrinking microbubble on gas hydrate formation. *The Journal of Physical Chemistry B* 107(10), 2171-2173.

Vadlakonda, B. and N. Mangadoddy (2017). Hydrodynamic study of two phase flow of column flotation using electrical resistance tomography and pressure probe techniques. *Separation and Purification Technology* 184, 168-187.

Wang, H., Y. Lin and W. Yang (2019). Investigation and analysis of a fluidized bed dryer by process tomography sensor. *Petroleum Science* 6(3), 1-12.

Wang, X. and X. Wu (2009). Gas-water stratified flow patterns from electromagnetic tomography. *Petroleum Science* 6(3), 254-258.

Wang, X., L. Guo, X. Zhang, H. Gu, C. Lin, D. Zhao and F. Guo (2005). Experimental study of severe slugging in pipeline-riser system. *Journal of Engineering Thermophysics* 26(5), 799-801 (in Chinese).

Xie, C., L. Guo, W. Li, *H.* Zhou and S. Zou (2017).The influence of backpressure on severe slugging in multiphase flow pipeline-riser systems. *Chemical Engineering Science* 163, 68-82.

Zhang, S., D. Wang, R. X. Duan and R. Duan (2015). Subsea hydrocarbon mixing transportation section of the pipeline slug flow serious problem. *Petrochemical Industry Technology* 22(7), 54-55, 42 (in Chinese).

Zhao, L., M. Lv, Z. Tang, Y. Shan, Z. Pan and Y. Sun (2018).Enhanced photo bio-reaction by multiscale bubbles. *Chemical Engineering Journal* 354, 304-313.

Zheng, G. H., J. P. Brill, and O. Shoham (1995). An Experimental Study of Two-Phase Slug Flow in Hilly Terrain Pipelines. *SPE Production & Facilities* 10(04), 233-240.